RSC Advances

ROYAL SOCIETY OF CHEMISTRY

www.rsc.org/advances

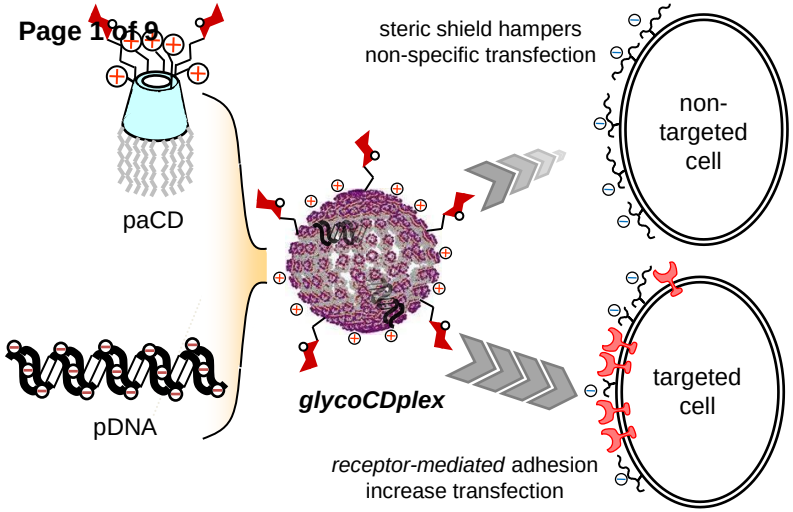

RSC Advances

ARTICLE

Harmonized tuning of nucleic acid and lectin binding properties with multivalent cyclodextrins for macrophage-selective gene delivery

Received 00th January 20xx,
Accepted 00th January 20xx

DOI: 10.1039/x0xx00000x

www.rsc.org/

Alejandro Méndez-Ardoy,[a,†] Alejandro Díaz-Moscoso,[b,‡] Carmen Ortiz Mellet,[a] Christophe Di Giorgio,[c,*] Pierre Vierling,[c] Juan M. Benito[b,*] and José M. García Fernández[b]

Polycationic amphiphilic cyclodextrins (paCDs) have been shown to behave as efficient non-viral gene carriers paralleling the efficacy of commercial vectors towards a variety of cell lines. Their molecular framework and modular design allow the installation of saccharidic antennae to promote specific carbohydrate-protein interactions, thus potentially endowing them with selective targeting abilities. Yet, the presence of these additional functionalities onto the polycationic cluster may hamper paCD self-assembly and nucleic acid condensation. In this report we describe the influence of paCD mannosylation extent on paCD-pDNA nanocomplex stability as well as the consequences of varying glycotope density on mannose-specific lectin recognition and gene delivery capabilites. The work aims at exploring the potential of this approach to optimize both properties in order to modulate cell transfection selectivity.

1. Introduction

Gene therapy (i.e. administering nucleic acid-based therapeutics to correct a particular cellular dysfunction) represents a promising alternative to conventional drugs due to the specific and predictable mode of action of polynucleotides.[1] Yet, it faces the drawback of the poor drug-likeness of nucleic acids, requiring purpose-conceived carriers, so-called vectors, to target their goal. Though their efficiency is still far from that of virus-based carriers, the advent of nanotechnology and the persisting safety concerns regarding the use of viral materials have fostered the design of a plethora of artificial gene vectors to cope with this task.[2] Molecular facial amphiphiles based on macrocyclic scaffolds,[3] among which polycationic amphipilic cyclodextrins (paCDs, Figure 1 left) are relevant representatives,[4,5] have turned particularly promising in this regard. paCDs undergo nucleic acid-templated self-assembling affording supramolecular nanocomplexes (CDplexes) that promote transfection with efficiencies that rival that of formulations prepared with commercial polycationic polymer (polyplexes) or lipid vectors (lipoplexes), but with no or much milder toxicity. Selectivity is however similarly low, since cell uptake of CDplexes, as for polyplexes and lipoplexes, relies essentially in non-specific electrostatic interactions.[6] Alternatively, exploiting specific ligand-receptor recognition events (e.g. between sugar epitopes and their complementary lectins) holds great promise for selectively targeting therapeutic genes.[7] The concept was put forward nearly 20 years ago,[8] but implementation with macromolecular systems is not that evident. Glycotargeting is presumed to arise from (i) the increase of the hydration shell of the carrier due to the hydrophilicity of the sugar motifs, which shields from non-specific (electrostatic) interactions, and (ii) specific receptor-mediated cell internalization (Figure 1, right). Recently, we have demonstrated that installation of a homogeneous glycomultivalent display on the cationic domain of paCDs selectively promoted gene delivery to cells expressing complementary lectin receptors.[9] Yet, the incorporation of glycoligands on the vector has a strong impact on the hydrophobic/hydrophilic balance and the hydrodynamic properties of the system, which may negatively affect self-assembling, nucleic acid compaction and, ultimately, transfections capabilities.[10,11] Harmonizing glycotope and cationic group densities to warrant biologically useful affinities towards both the target lectin and the nucleic acid cargo is thus critical for those channels.

[a] Departamento de Química Orgánica, Facultad de Química, Univ. Sevilla, C/ Prof. García González 1, E-41012 Sevilla, Spain. E-mail: mellet@us.es.
[b] Instituto de Investigaciones Químicas, CSIC – Univ. Sevilla, Américo Vespucio 49, E-41092 Sevilla, Spain. E-mail: jogarcia@iiq.csic.es.
[c] Institut de Chimie de Nice, ICN - Université de Nice Sophia Antipolis – CNRS UMR 7272, 28, Avenue de Valrose, F-06100 Nice, France. E-mail: Christophe.DI-GIORGIO@unice.fr
† Present address: Université de Bordeaux, Institute de Sciences Moléculaires (ISM), Nanostructures Organiques, 33405 Talence, France.
‡ Present address: Institute of Chemical Research of Catalonia (ICIQ), 43007 Tarragona, Spain.
Electronic Supplementary Information (ESI) available: Experimental details, NMR and ESI-MS spectra, and dynamic light scattering (DLS) measurement figures. See DOI: 10.1039/x0xx00000x

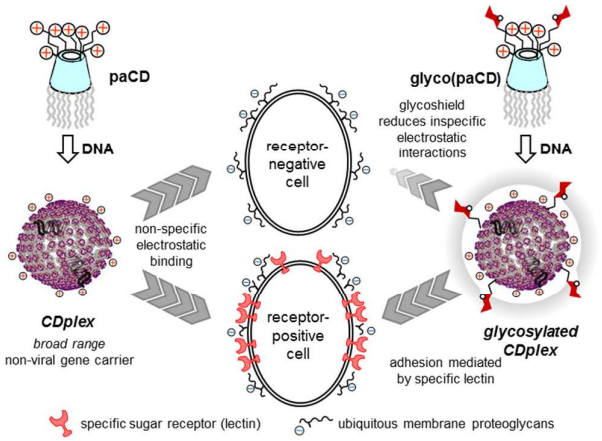

Figure 1. Schematic representation of the mechanisms involved in cell-membrane binding of CDplexes: naked CDplexes (left) exploit non-specific electrostatic interactions with negatively-charged cell membrane proteoglycans. Conversely, in glycoCDplexes (right) these interactions are hampered by the heavier solvation of the carbohydrate shield, thus adhesion is mostly dependent on specific multivalent interactions with the appropriate receptor (lectin).

In this paper, we report the synthesis of a series of statistically mannosylated paCDs featuring variable relative proportions of sugar and protonable amino centres and a preliminary assessment of how mannosylation extent modulates the nucleic acid condensing capacity, the dynamics and stability of the resulting glycoCDplexes, the binding affinity to mannose-specific receptors and the transfection efficiency towards macrophage mannose receptor (MMR) positive (RAW 264.7) and negative (BNL-CL2 and COS-7) cell lines.

2. Results and discussion

2.1. Selection criteria and synthesis

Compounds **1a**[12a] and **2a**[12b] (Scheme 1), featuring very similar structures but subtle vector performance disparities, were selected as paCD scaffolds to investigate the effect of increasing mannosylation degrees on DNA complexing abilities and MMR recognition properties. The transfection efficiency of pDNA complexes formulated with triazol-armed paCD **1a** is optimal at a nitrogen/phosphorus (N/P) ratio of 10.[13] Thiourea-tethered paCD **2a**, on the other hand, achieves similar expression levels at a lower N/P (5), which is attributed to the privileged phosphate binding ability of the 2-aminoethylthiourea segments on the cationic cluster.[12b]

Cyclodextrin scaffolds **1a** and **2a** were conjugated with 2-(α-D-mannopyranosyloxy)ethyl isothiocyanate (**3**)[14] using thiourea-forming ligation chemistry (Scheme 1). Each individual coupling reaction results then in the replacement of a cationizable centre in the vector by a neutral biorecognizable glycotope. Reaction with increasing amounts of isothiocyanate **3** (5 to 50% relative to the paCD primary amino groups), followed by purification by size exclusion chromatography, furnished two series of paCDs with different degrees of mannosylation (**1b**-**e** and **2b**-**e**, respectively). ESI-MS and ^{1}H NMR spectroscopy confirmed quantitative mannoside incorporation in all cases (see Supplementary Information).

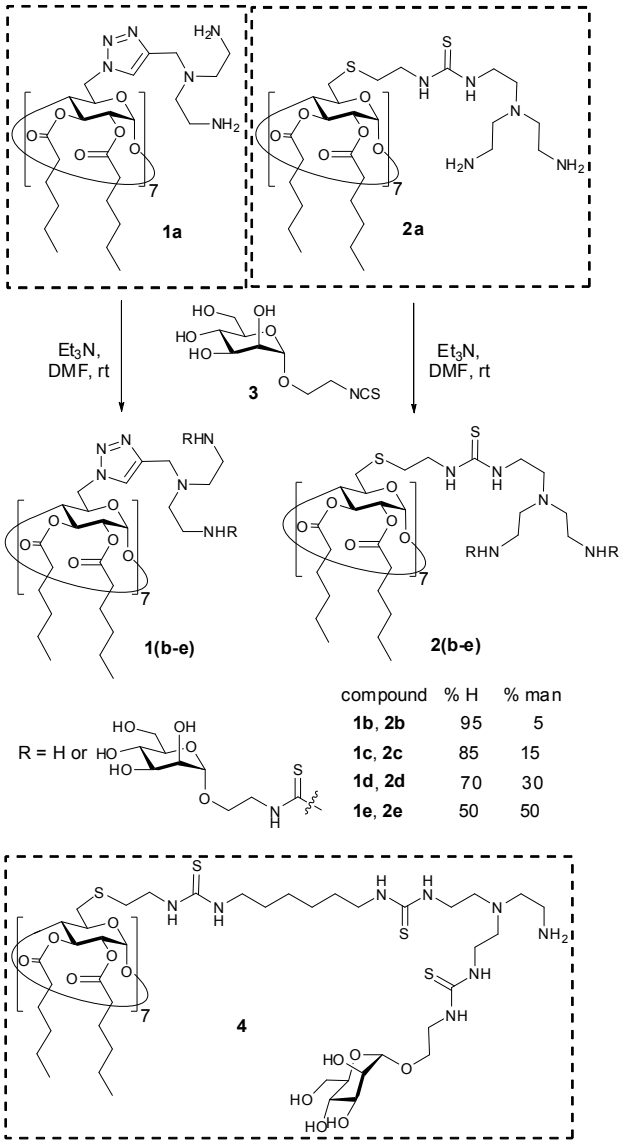

compound	% H	% man
1b, **2b**	95	5
1c, **2c**	85	15
1d, **2d**	70	30
1e, **2e**	50	50

Scheme 1. Synthesis of statistically mannosylated paCDs from **1a** and **2a** and structure of the homogenously mannosylated derivative **4** used as positive control in macrophage adhesion experiments.

The above multiconjugation strategy provides a very convenient method to modulate the coating sugar content of the paCD vectors while significantly reducing the synthetic effort as compared with regioselective synthetic schemes previously implemented, e.g. for the synthesis of the heptamannosylated glyco(paCD) **4** (Scheme 1).[9] Although it obviously affords polydisperse mixtures of statistically glycosylates adducts, it is presumed that differences in glycocluster topology at the molecular level would be blurred when considering the glycocoating corona in the nanocomplexes after self-assembling with pDNA.[7] Indeed, the scenario is very similar to that encounter for statistic glycosylation of polymeric or dendritic scaffolds, a routinely used strategy to generate multivalency.[10,15,16] Glycotope density is then expected to become the main parameter

influencing specific lectin recognition and gene delivery properties.

2.2. Self-assembling capabilities

The influence of the mannosylation degree in the pDNA (luciferase-encoding pTG11236 plasmid) complexing capabilities of paCDs **1a**-**e** and **2a**-**e** was first screened by agarose gel electrophoresis migration experiments at different N/P ratios (1, 2, 5, and 10). No remarkable differences were noticed between the behaviour of triazol- (**1a**-**e**; Figure 2, left column) and thiourea-tethered (**2a**-**e**; Figure 2, right column) series. In general, mannosylation progressively decreases the ability to inhibit pDNA electrophoretic mobility of the paCDs, which is better evidenced in the thiourea-tethered series (Figure 2, right column). Nevertheless, regardless of their mannosylation degree, all glyco(paCDs) inhibited electrophoretic mobility of pDNA at N/P ratios above 2. Comparatively, the pDNA protection against the intercalating agent ethidium bromide is more influenced by mannosylation. While pDNA is already inaccessible to ethidium bromide at N/P ≥2 in formulations with **1a** and **2a** (Figure 2, first row), N/P 5 ratios are required for most mannosylated adducts to attain the same protection, mounting up to N/P 10 for the more heavily mannosylated triazol-linked glyco(paCD) **1e** (50% mannosylation). Although electrostatic interactions with the plasmid are preserved, compaction is probably hampered as a consequence of the higher swelling capabilities imparted by the hydrophilic sugar residues.

The hydrodynamic size and ζ-potential of glycoCDplexes formulated at N/P values 5 and 10 were next measured by dynamic light scattering (DLS) and mixed-mode measurement-phase analysis light scattering (M3-PALS), respectively. Dispersion of paCDs in a solution of pDNA in water furnished single populations of rather homogenous nanoparticles (polydispersity index ≈ 0.2) in all cases. (Glyco)CDplexes obtained from triazol-containing paCDs **1a**-**e** evidenced a gradual, though subtle, increase in size and a parallel decrease in ζ-potential upon increasing the mannosylation degree, which was especially noticeable for formulations at N/P 10 (Figure 3, left). It is worth mentioning that although an increase in sugar valency is accompanied by a decrease in the number of protonable amino groups in the glyco(paCD) conjugates, this has been compensated by normalizing at the same N/P ratio. The observed trend is probably due to the increase in the thickness of the hydration shell with heavier mannosylation, which is also expected to shield the nanoparticle surface charge to some extent. The increase in size upon glycosylation was less evident in the thiourea-tethered conjugates **2a**-**e** (Figure 3, right). In this case, a significant decrease in ζ-potential was already observed for the vector with the lower glycosylation rate (**2b**, 5% mannosylation), further increases in valency having much more modest consequences. It is hypothesized that the higher flexibility of the linker in this series allows a better accommodation of the mannosyl residues in the glycoCDplexes, minimizing the impact of glycosylation density variations.

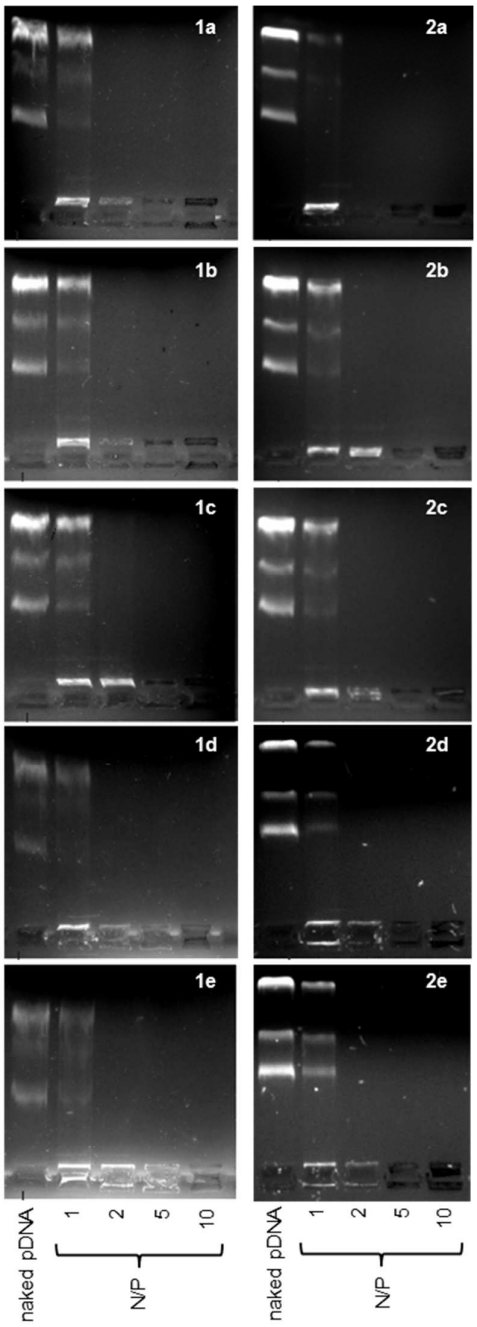

Figure 2. pDNA retardation in agarose gel vs mannosylation degree (from top to bottom, 0 to 50% of available primary amino groups, respectively) and N/P ratio (0 to 10, lanes 1 to 5 in each picture). Left and right columns collect data for paCD **1a**-**e** and **2a**-**e**, respectively.

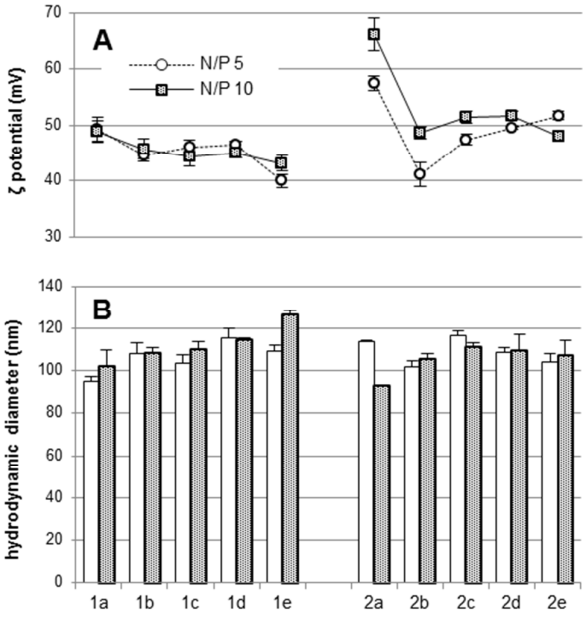

Figure 3. ζ-Potential (A) and hydrodynamic diameter (B) of statistically mannosylated CDplexes formulated at N/P 5 (white circles and empty bars) and 10 (filled squares and dotted bars) determined by M3-PALS and DLS, respectively.

The effect of mannosylation extent on the size and stability of the nanocomplexes formulated with the paCD derivatives **1a**-**e** and **2a**-**e** and pDNA in saline medium (up to 150 mM NaCl) was next investigated to further assess their behavior under physiological conditions. As a general trend, mannosylation attenuated the effect of saline stress on the colloidal stability of glycoCDplexes, as seen from the less pronounced differences in size (Supplementary Information, Fig. S11). This result is in agreement with previous reports on glycocluster-based vectors[10,17] and reinforces the notion that sugar coating prevents non-specific aggregation phenomena, probably by endowing the nanoparticles with a thicker hydration shell. The accessibility of ethidium bromide to the pDNA cargo in the most heavily mannosylated glycoCDplexes (e.g. **1e**) increases under saline stress (Supplementary Information, Fig. S12), also pointing to a non-optimal hydrophilic/hydrophobic balance at such high mannose coating densities.

2.3. Alveolar macrophage adhesion

The average mannose valencies of the paCDs prepared and evaluated in this work, taken as individual entities, are 0, 0.7, 2.1, 4.2 and 7 for **1a** and **2a** to **1e** and **2e**, respectively. According to results reported for non-amphiphlic CD-scaffolded glycoclusters,[18] a significant multivalent effect would be expected only for the later derivatives. Yet, after supramolecular self-assembling in the presence of pDNA a hyper-valent display of mannosyl epitopes will be generated at the surface of the glycoCDplexes formulated with **1b**-**e** and **2b**-**e**. We were particularly interested at investigating the minimum mannosylation rate leading to functional DNA nanocomplexes capable of eliciting a biologically significant binding to cells expressing the macrophage mannose receptor. For such purpose, glycoCDplexes were formulated using pDNA labelled with the fluorescent probe YOYO-1 at N/P ratios 5 and 10. The ability of these particles to adhere the surface of alveolar peritoneal macrophages at 4 ºC (to prevent endocytosis) was assessed by fluorescence intensity measurements (Figure 4).[19] At the lower N/P ratio, a significant increase in fluorescence was noticed even at relatively low mannosylation ratios as compared to negative controls (naked pDNA, non-glycosylated CDplexes formulated with paCDs **1a** and **2a**, and polyplexes formulated with the commercial vector JetPEI).[20] Interestingly, fluorescence intensity plateaued at ca. 15-30% mannosylation (**1c**, **2c** and **1d**, **2d**), with residual increase at higher glycan ratios. Indeed, similar macrophage adhesion levels were obtained for the positive control, the homogeneously 50% mannosylated paCD **4** (Scheme 1). At N/P 10, though the tendency is similar, the contrast is lower, due to the higher background of non-specific electrostatic interactions. As it could be expected, the higher the cationic content, the lower the contribution of specific interactions to the overall adhesion process, a phenomenon already described for a variety of cationic gene carriers.[21]

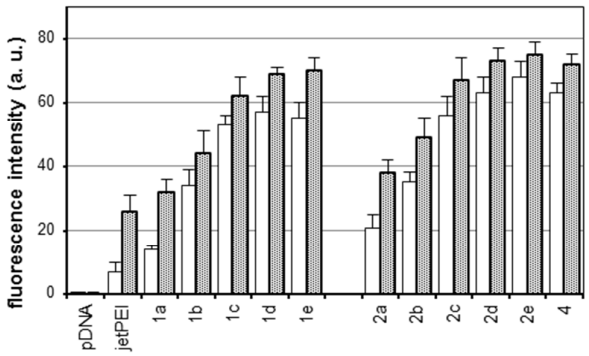

Figure 4. Adhesion to alveolar peritoneal macrophages (mice) of statistically mannosylated CDplexes **1a**-**e** and **2a**-**e** formulated at N/P ratio 5 (white bars) and 10 (grey bars) vs. naked pDNA. JetPEI polyplexes and **4**:pDNA CDplexes formulated at the same N/P ratio were used as negative and positive controls, respectively.

To confirm the specificity of the interactions at play, the above experiments were run in the presence of native and mannosylated-BSA (Man-BSA) as competing agents, using the optimal N/P ratio 5. A mannose concentration-dependent inhibition of glycoCDplex adhesion to the macrophages was observed for the later, with fluorescence intensity values reduced to basal levels in the presence of 1 mg·mL^{-1} of Man-BSA (Figure 5). On the other hand, native BSA minimally affected adhesion. Neither BSA nor Man-BSA significantly affected the adhesion of JetPEI polyplexes and non-mannosylated CDplexes to macrophages, altogether strongly supporting the involvement of specific mannose-MMR recognition in the adhesion of the glycoCDplexes formulated with **1b**-**e** and **2b**-**e** to the macrophages.

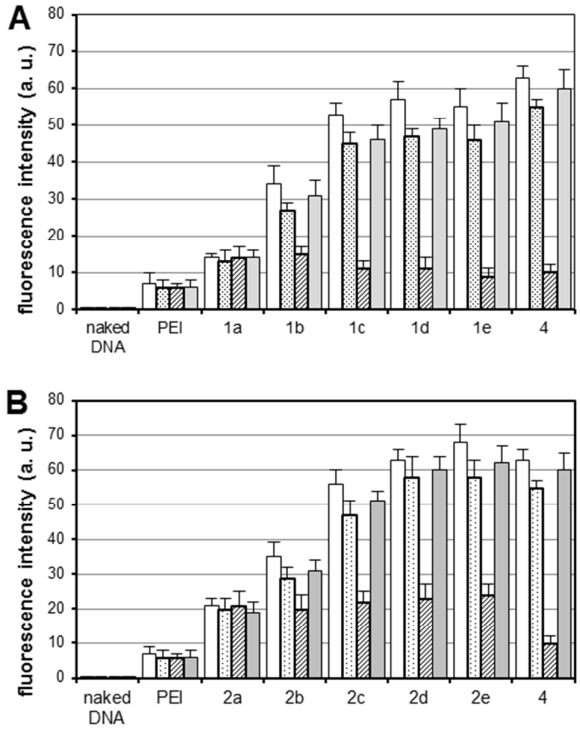

Figure 5. Adhesion of CDplexes **1a**-**e** (A) and **2a**-**e** (B) formulated at N/P 5 in the absence of BSA (white bars), in the presence of mannosylated-BSA (0.1 and 1 mg·mL^{-1}, dotted and slashed bars, respectively) or in the presence of native BSA (grey bars). JetPEI polyplexes and **4**:pDNA CDplexes formulated at the same N/P ratio were used as negative and positive controls, respectively.

2.4. Cell transfection

CDplexes formulated at N/P 5 with luciferase-encoding pDNA (pTG11236) and the multivalent paCD vectors having 15 and 30% of the primary amino groups replaced by mannosyl antennae (**1c**, **2c** and **1d**, **2d**, respectively) were selected for cell transfection assays. According to the previously discussed results, these formulations exhibit the best balance between pDNA protection, colloidal stability and MMR-binding efficiency, which was expected to maximize receptor-mediated versus non-specific (electrostatic-mediated) cell uptake. Transfection was monitored in MMR-positive mouse leukaemic monocyte macrophages (RAW 264.7) and in MMR-devoid embryonic murine hepatocytes (BNL-CL2) and African green monkey kidney fibroblasts (COS-7). In all three cell lines and for all formulation, cell viabilities were determined to be above 80%. The corresponding luciferase expression data are plotted in Figure 6. Naked pDNA and JetPEI polyplexes formulated at N/P 5 were used as negative and positive controls, respectively (see Supplementary Information for experimental details).

The graphs depict two different scenarios depending on the presence of triazol (**1a**, **1c** and **1d**) or thiourea linkers (**2a**, **2c** and **2d**). In the triazol-tethered series, the transfection efficiency of the non-mannosylated CDplexes formulated with paCD **1a** at N/P 5 is very poor in the three cell lines, only marginally improving that of naked pDNA. Indeed, previous results have shown that triazol-tethered paCD efficiency peaks at higher N/P ratios, ca. 10.[13] The mannosylated vectors **1c** and **1d** behaved similarly poorly in the MMR-devoid BNL-CL2 and COS-7 cell lines (Figure 6A). Rewardingly a significant enhancement of the transfection efficiency relative to the control was observed in MMR-expressing RAW264.7 cells (29- and 12-folds for glycoCDplexes formulated with **1c** and **1d**, respectively). A direct comparison of the data for the three cell lines reveals a 5 to 12-fold higher protein expression in MMR-expressing as compared to MMR-devoid cells (Figure 7A).

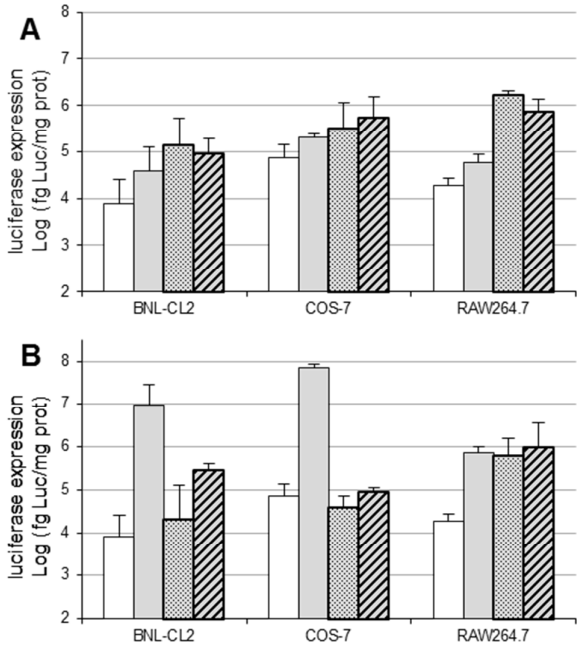

Figure 6. Transfection efficiency in terms of luciferase expression in BNL-CL2, COS-7, and RAW 264.7 cells for CDplexes formulated at N/P 5 with triazol-tethered (**1a**, grey bars; **1c**, dotted bars; **1d**, slashed bars; panel A) and thiourea-tethered (**2a**, grey bars; **2c**, dotted bars; **2d**, slashed bars; panel B) paCDs. Naked pDNA was used as negative control.

CDplexes formulated with the thiourea-tethered paCD **2a** at N/P 5 already elicited relevant levels of luciferase activity in all three cell lines. Upon conjugation with mannose, transfection levels dropped very significantly in MMR-devoid BNL-CL2 and COS-7 cells (Figure 6B). In contrast, transfection of RAW264.7 macrophages with the mannosylated conjugates **2c** and **2d** remained unaltered, probably because the detrimental effect due to attenuation of electrostatic interactions is compensated by activation of MMR-mediated cell uptake mechanisms. Even though a net enhancement in macrophage transfection efficiency is not achieved, off-target effects are very significantly reduced, imparting cell selectivity. Thus, while the parent paCD vector **2a** promoted transfection of the hepatocyte and fibroblast cells with 13- and 100-fold higher efficiencies as compared with macrophages, the corresponding conjugate **2c**, with a 15% mannose incorporation, transfected preferentially macrophages, with 31-fold and 16-fold higher

efficiency as compared with hepatocytes and fibroblasts, respectively (Figure 7B). This means a reversion of the cell selectivity in favour of the MMR-expressing cells by a factor of 400 to 1600.

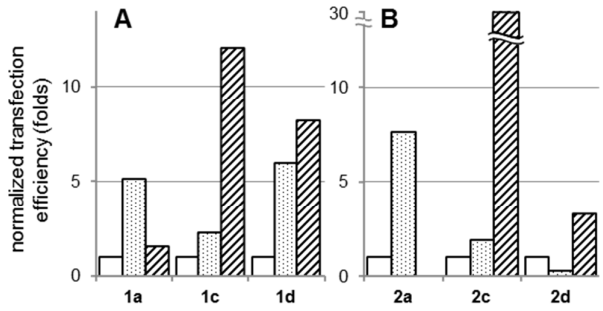

Figure 7. Normalized transfection efficiency of CDplexes formulated at N/P 5 with triazol-tethered (**1a**, **1c** and **1d**; A) and thiourea-tethered (**2a**, **2c** and **2d**; B) paCDs in BNL-CL2 (white bars), COS-7 (dotted bars), and RAW 264.7 (slashed bars) cells. Luciferase expression levels in BNL-CL2 cells have been arbitrarily given the value 1, so that the values for COS-7 and RAW 264.7 cells represent transfection potency (in folds) relative to the former.

4. Conclusions

The results presented in this work demonstrate that the installation of defined proportions of saccharidic epitopes onto molecular polycationic amphiphilic CD scaffolds can be used to modulate their DNA-templated self-assembling capabilities and the functional properties of the resulting nanocomplexes. Self-assembling of glyco(paCDs) leads to amplification of interactions with complementary lectin receptors by generating a multivalent glyocodisplay at the nanoparticles surface. Glycocoating additionally shields the positive charge of glycoCDplexes, decreasing the non-specific electrostatic interactions with proteoglycans at the cell surface. Altogether glyco(paCDs) can be exploited to enhance cell transfection selectivities by judiciously tuning the nucleic acid and lectin binding properties, as exemplified here for macrophages, after synchronized adjustment of the positive charge density and the glycosylation extent.

5. Experimental

5.1. General methods

Reagents and solvents were purchased from commercial sources and used without further purification. NMR spectra were recorded at 500 MHz. 2D COSY, 1D TOCSY experiments were used to assist on NMR assignments. Gel permeation chromatography was carried out on Sephadex G-25 (GE Healthcare Life Sciences). Electrospray mass spectra (ESIMS) were obtained with a Bruker Esquire6000 instrument. Compounds **1a**,[12a] **2a**,[12b] **3**,[14] and **4**[9] were synthesized as previously reported.

5.2. Synthesis

Procedure for statistical mannosylation of paCDs **1a** and **2a**: To a solution of paCD (12 µmol) and Et_3N (47 µL, 0.34 mmol, 2 eq) in dry DMF (5 mL), a solution of 2-isothiocyanatoethyl α-D-mannopyranoside 3 (2.2 mg, 6.7 mg, 13.3 mg or 22.3 mg for 0.05, 0.15, 0.30 or 0.50 eq per primary amino group, respectively) in DMF (5 mL) was added and the solution was stirred overnight at room temperature. The solvent was removed under vacuum and the residue was purified by size exclusion chromatography (Sephadex G-25) using water as eluent. The purified compound was dissolved in diluted HCl 0.1 N and freeze-dried to give a white foam in nearly quantitative yields. For detailed characterization see Supplementary Information section.

5.3. Preparation of complexes composed of paCDs and pDNA pTG11236

The plasmid pTG11236[22] (pCMV-SV40-luciferase-SV40pA) employed for the preparation of the DNA complexes and for transfection assay is a plasmid of 5739 bp (base pairs). The quantities of each formulation were calculated according to the DNA concentration (0.1 mg·mL^{-1}, 303 µM phosphate), the N/P ratio, the molar weight and the number of positive charges in the paCD derivative or cationic polymer (JetPEI®).[20] Experiments were performed for N/P 1, 2, 5 and 10. Concerning the preparation of the DNA complexes from paCD derivatives and JetPEI, pDNA was diluted in HEPES (20 mM, pH 7.4) to a final concentration of 303 µM (1 mg·mL^{-1}), then the desired amount of CD derivative was added from a 20 mg·mL^{-1} stock solution (DMSO-water, 1:2, v:v) and JetPEI was added from a 0.1 M stock solution (water). Final concentration of DMSO never exceeded 2% in these preparations. The preparation was vortexed for 2 h and used for characterization or transfection experiments.

5.4. Agarose gel electrophoresis

Each CD derivative/DNA sample (20 µL, 0.4 µg of plasmid) was electrophoresed for about 30 min under 150 V through a 0.8% agarose gel in TAE 1X (Tris-acetate-EDTA) buffer and stained by spreading an ethidium bromide (Sigma) solution in TAE buffer (20 µL ethidium bromide of a 10 mg·mL^{-1} solution in 200 mL TAE). The DNA was then visualized after photographing on an UV transilluminator.

5.5. Particle size and ζ potential measurements

The hydrodynamic diameters of the vesicles formed from the paCDs were measured by Dynamic Light Scattering (DLS) at 633 nm on a Nanosizer S DLS instrument (Malvern Instruments) at 25 ºC and at a detection angle of 173º. All the measurements were performed in triplicate. Data were analysed using the multimodal number distribution software included in the instrument. Results are given as volume distribution of the major population by the mean diameter with its standard deviation. Statistical analysis of the particle size was performed using a student's test (with two-sample unequal variance and two distribution tails). The ζ potential measurements were also performed in the same instrument

using 'Mixed Mode Measurement' phase analysis light scattering (M3-PALS). M3 consists of both slow field reversal and fast field reversal measurements, hence the name 'Mixed Mode Measurement' that improves accuracy and resolution. PALS is a variation of laser Doppler velocimetry that uses the phase shift (i.e. frequency x time) instead of the frequency shift to determine electrophoretic mobilities and hence convert them into zeta potentials. The following specifications were applied: sampling time, automatic; number of measurements, 3 per sample; medium viscosity, 1.054 cP; medium dielectric constant, 80; temperature, 25 °C; beam mode F(Ka)) 1.5 (Smoluchowsky). Experiments were run by in triplicate.

5.6. Salt-induced CDplex dissociation assays

CDplexes were prepared as described above in order to obtain a final DNA concentration of 60 µM after adding a volume (representing 10% of total volume) of a NaCl solution in HEPES (in order to obtain a final NaCl concentration of 0, 50, 150 and 250 mM), and a volume (representing 2% of total volume) of a 100 µM ethidium bromide solution in DMSO. After adding, each preparation was vortexed for 15 minutes before fluorescence measurements. Each CDplex formulation was arrayed in triplicate into a white flat-bottom 96-well plate. The ethidium bromide fluorescence of each sample was measured with a luminometer (GENIOS PRO, Tecan France S.A.; excitation 485 nm, emission 590 nm). The relative ethidium bromide exclusion (% DNA excluded to ethidium bromide) was determined by the following relationship:

$$Relative_{(EtBr\ exclusion)} = 1 - [(F_{sample} - F_{blank}) / [F_{DNAonly} - F_{blank})]$$

5.7. Alveolar macrophage adhesion assays

For evaluation of the interaction of YOYO-1-labeled CDplexes with alveolar macrophages, the procedure reported by Muller and Schuber[19a] for mannosylated liposomes was adapted. Briefly, resident peritoneal macrophages were obtained from female Balb/c mice (6 to 8 weeks old) and maintained in Dulbecco's modified Eagle's medium (DMEM; Gibco-BRL) supplemented with 10% decomplemented fetal calf serum (FCS; Sigma) containing heparin (5 U/mL). The cell number was adjusted to 10^6 cells·mL^{-1} and the suspension was platted (final volume 1 mL) in multi-well plates. After 2 h in a humidified atmosphere of 5% CO_2 in air (final pH 7.4), non-adherent cells were eliminated by rinsing the dishes three times with PBS. The adherent cells, 24 h after their isolation, were fed with fresh serum-less DMEM and incubated with CD-pDNA nanocomplexes, PEI polyplexes and naked DNA (control) at similar DNA concentration used in transfection assays. After the incubation time, the medium was pipetted-off and the cells washed four times with cold PBS (4 ºC). The fluorescent tag associated to the cells was measured fluorimetrically (Perkin Elmer luminescence spectrometer LS50B, excitation at 491 nm and monitoring emission at 509 nm) after cell digestion in 1 mL PBS containing 0.1% of emulphogene BC-720, and scraping with a rubber policeman. Experiments were run in duplicate, and results did not differ more than 10%.

5.8. In vitro transfection

Twenty-four hours before transfection, BNL-CL2, COS-7, and RAW264.7 cells were grown at a density of 2 x 10^4 cells/well in a 96-well plates in Dulbelco modified Eagle culture medium (DMEM; Gibco-BRL) containing 10% foetal calf serum (FCS; Sigma) in a wet (37 ºC) and 5% CO_2/95% air atmosphere. The complexes CD derivative/DNA or PEI/DNA polyplexes were diluted to 100 µL in DMEM in order to have 0.5 µg of DNA in the preparation. The culture medium was removed and replaced by these 100 µL of complexes in DMEM. After 4 h and 24 h, 50 and 100 µL of DMEM supplemented with 30% and 10% FCS, respectively, were added. After 48 h, the transfection was stopped, the culture medium was discarded, and the cells washed twice with 100 µL of PBS and lysed with 50 µL of lysis buffer (Promega, Charbonnières, France). The lysates were frozen at -32 ºC, before the analysis of luciferase activity. This measurement was performed in a LB96P luminometer (BERTHOLD, France) in dynamic mode, for 10 s on 10 mL on the lysis mixture and using the "luciferase" determination system (Promega) in 96-well plates. The total protein concentration per well was determined by the BCA test (Pierce, MontluÇon, France). Luciferase activity was calculated as femtograms (fg) of luciferase per mg of protein. The percentage of cell viability of the nanocomplexes was calculated as the ratio of the total protein amount per well of the transfected cells relative to that measured for untreated cells x 100%.

6. Acknowledgements

This work was supported by the Spanish Ministerio de Economía y Competitividad (MinECo; contract number SAF2013-44021-R), the Junta de Andalucía (Proyecto de Investigación de Excelencia FQM-1467), the Fondo Europeo de Desarrollo Regional (FEDER-Unión Europea), the Fondo Social Europeo (FSE) the CSIC, the CNRS, and FUSINT (CNRS project). A.M.-A. and A.D.-M. are grateful to MinECo and CSIC, respectively, for pre-doctoral fellowships.

Notes and references

1 V. K. Sharma, P. Rungta and A. K. Prasad, *RSC Adv.*, 2014, **4**, 16618.

2 (*a*) M. Elsabahy, A. Nazarali and M. Foldvari, *Curr. Drug Deliv.*, 2011, **8**, 235; (*b*) M. A. Mintzer and E. E. Simanek, *Chem. Rev.*, 2009, **109**, 259; (c) C. H. Jones, C.-H. Chen, A. Ravikrishnan, S. Rane and B. A. Pfeifer, *Mol. Pharmaceutics*, 2013, **10**, 4082.

3 (*a*) B. J. Ravoo and R. Darcy, *Angew. Chem. Int. Ed.* 2000, **39**, 4324; (*b*) C. Ortiz Mellet, J. M. Benito and J. M. García Fernández, *Chem. – Eur. J.*, 2010, **16**, 6728; (*c*) V. Bagnacani, V. Franceschi, M. Bassi, M. Lomazzi, G. Donofrio, F. Sansone, A. Casnati and R. Ungaro, *Nat. Commun.*, 2013, ***4***, 1721; (*d*) V. Bagnacani, V. F. L. Fantuzzi, F. Sansone, G. Donofrio, A. Casnati and R. Ungaro, *Bioconjugate Chem.*, 2012, **23**, 993; (*e*) L. Gallego-Yerga, M. Lomazzi, V. Franceschi, F. Sansone, C. Ortiz Mellet, G. Donofrio, A. Casnati and J. M. García Fernández, *Org. Biomol. Chem.*, 2015, **13**, 1708.

4 (*a*) B. M. D. C. Godinho, D. J. McCarthy, C. Torres-Fuentes, C. J. Beltrán, J. McCarthy, A. Quinlan, J. R. Ogier, R. Darcy, C. M. O'Driscoll and J. F. Cryan, *Biomaterials*, 2014, **35**, 489; (*b*) J. McCarthy, M. J. O'Neill, L. Bourre, D. Walsh, A. Quinlan, G. Hurley, J. Ogier, F. Shanahan, S. Melgar, R. Darcy and C. M. O'Driscoll, *J. Control. Release*, 2013, **168**, 28; (*c*) A. M. O'Mahony, B. M. D. C. Godinho, J. Ogier, M. Devocelle, R. Darcy, J. F. Cryan and C. M. O'Driscoll, *ACS Chem. Neurosci.*, 2012, **3**, 744; (d) V. Villari, A. Mazzaglia, R. Darcy, C. M. O'Driscoll and N. Micalli, *Biomacromolecules*, 2013, **14**, 811.

5 (*a*) N. Guilloteau, C. Bienvenu, C. Charrat, J.L. Jiménez Blanco, A. Díaz-Moscoso, C. Ortiz Mellet, J. M. García Fernández, P. Vierling and C. Di Giorgio, *RSC Adv.*, 2015, **5**, 29135; (*b*) C. Aranda, K. Urbiola, A. Méndez Ardoy, J. M. García Fernández, C. Ortiz Mellet and C. Tros de Ilarduya, *Eur. J. Pharm. Biopharm.*, 2013, **85**, 390; (*c*) A. Martínez, C. Bienvenu, J. L. Jiménez Blanco, P. Vierling, C. Ortiz Mellet, J. M. García Fernández and C. Di Giorgio, *J. Org. Chem.*, 2013, **78**, 8143; (*d*) C. Bienvenu, A. Martínez, J. L. Jiménez Blanco, C. Di Giorgio, P. Vierling, C. Ortiz Mellet, J. Defaye and J. M. García Fernández, *Org. Biomol. Chem.*, 2012, **10**, 5570.

6 (*a*) L. Gallego-Yerga, M. J. González-Alvarez, N. Mayordomo, F. Santoyo-González, J. M. Benito, C. Ortiz Mellet, F. Mendicuti and J. M. García Fernández, *Chem. – Eur. J.*, 2014, **20**, 6622; (*b*) L. Gallego-Yerga L. Blanco-Fernández, K. Urbiola, T. Carmona, G. Marcelo, J. M. Benito, F. Mendicuti, C. Tros de Ilarduya, C. Ortiz Mellet and J. M. García Fernández, *Chem. – Eur. J.*, 2015, **21**, in press, DOI: 10.1002/chem.201501678.

7 S. Kawakami and M. Hashida, *J. Control. Release*, 2014, **190**, 542.

8 (*a*) P. Erbacher, A. C. Roche, M. Monsigny and P. Midoux, *Bioconjugate Chem.*, 1995, **6**, 401; (*b*) J. S. Remy, A. Kichler, V. Mordvinov, F. Schuber and J. P. Behr, *Proc. Natl. Acad. Sci.*, 1995, **92**, 1744; (*c*) T. Ferkol, J. C. Perales, F. Mularo and R. W. Hanson, *Proc. Natl. Acad. Sci.*, 1996, **93**, 101.

9 A. Díaz-Moscoso, N. Guilloteau, C. Bienvenu, A. Méndez-Ardoy, J. L. Jiménez Blanco, J. M. Benito, L. Le Gourrierec, C. Di Giorgio, P. Vierling, J. Defaye, C. Ortiz Mellet and J. M. García Fernández, *Biomaterials*, 2011, **32**, 7263.

10 S. M. D'Addio, S. Baldassano, L. Shi, L. Cheung, D. H. Adamson, M. Bruzek, J. E. Anthony, D. L. Laskin, P. J. Sinko, R. K. Prud'homme, *J. Control. Release*, 2013, **138**, 41.

11 E. M. Aguilar Moncayo, N. Guilloteau, C. Bienvenu, J. L. Jiménez Blanco, C. Di Giorgio, P. Vierling, J. M. Benito, C. Ortiz Mellet and J. M. García Fernández, *New J. Chem.*, 2014, **38**, 5215.

12 (*a*) A. Méndez-Ardoy, M. Gómez-García, C. Ortiz-Mellet, N. Sevillano, M. D. Girón, R. Salto, F. Santoyo-González and J. M. García Fernández, *Org. Biomol. Chem.*, 2009, **7**, 2681; (*b*) A. Díaz-Moscoso, L. Le Gourrierec, M. Gómez-García, J. M. Benito, P. Balbuena, F. Ortega-Caballero, N. Guilloteau, C. Di Giorgio, P. Vierling, J. Defaye, C. Ortiz Mellet and J. M. García Fernández, *Chem. – Eur. J.*, 2009, **15**, 12871.

13 A. Mendez-Ardoy, N. Guilloteau, C. Di Giorgio, P. Vierling, F. Santoyo-González, C. Ortiz Mellet and J. M. García Fernández, *J. Org. Chem.*, 2011, **76**, 5882.

14 C. Grabosch, K. Kolbe and T. K. Lindhorst, *ChemBioChem*, 2012, **13**, 1874.

15 (*a*) N. Symens, A. Méndez-Ardoy, A. Díaz-Moscoso, E. Sánchez-Fernández, K. Remaut, J. Demeester, J. M. García Fernández, S. C. De Smedt and J. Rejman, *Bioconjugate Chem.*, 2012, **23**, 1276; (*b*) W. Yeeprae, S. Kawakami, F. Yamashita and M. Hashida, *J. Control. Release*, 2006, **114**, 193; (*c*) L. Raviv, M. Jaron-Mendelson and A. David, *Mol. Pharmaceutics*, 2015, **12**, 453; (*d*) S. Chu, C. Tang and C. Yin, *Biomaterials*, 2015, **52**, 229.

16 (*a*) H. Arima, K. Motoyama and T. Higashi, *Adv. Drug Deliv. Rev.*, 2013, **65**, 1204; (*b*) L. L. Kiessling and J. C. Grim, *Chem. Soc. Rev.* 2013, **42**, 4476.

17 O. Hayashida, K. Mizuki, K. Akagi, A. Matsuo, T. Kanamori, T. Nakai, S. Sando and Y. Aoyama, *J. Am. Chem. Soc.*, 2003, **125**, 594.

18 A. Martínez, C. Ortiz Mellet and J. M. García Fernández, *Chem. Soc. Rev.*, 2013, **42**, 4746.

19 (*a*) C. D. Muller and F. Schuber, *Biochim. Biophys. Acta*, 1989, **986**, 97; (*b*) J. Rodríguez-Lavado, M. de la Mata, J. L. Jiménez-Blanco, M. I. García-Moreno, J. M. Benito, A. Díaz-Quintana, J. A. Sánchez-Alcázar, K. Higaki, E. Nanba, K. Ohno, Y. Suzuki, C. Ortiz Mellet and J. M. García Fernández, *Org. Bimol. Chem.*, 2014, **12**, 2289.

20 (*a*) M.-H. Louis, S. Dutoit, Y. Denoux, P. Erbacher, E. Deslandes, J.-P. Behr, P. Gauduchon and L. Poulain, *Cancer Gene Ther.*, 2006, **13**, 367; (*b*) O. Boussif, F. Lezoualc'h, M. A. Zanta, M. D. Mergny, D. Scherman, B. Demeneix and J.-P. Behr, *Proc. Natl. Acad. Sci. USA*, 1995, **92**, 7297.

21 (*a*) E. Letrou-Bonneval, R. Chèvre, O. Lambert, P. Costet, C. André, C. Tellier and B. Pitard, *J. Gene Med.*, 2008, **10**, 1198; (*b*) J. S. Remy, A. Kichler, V. Mordvinov, F. Schuber and J.-P. Behr, *Proc. Natl. Acad. Sci. USA*, 1995, **92**, 1744.

22 (*a*) J. Gaucheron, C. Boulanger, C. Santaella, N. Sbirrazzuoli, O. Boussif and P. Vierling, *Bioconjugate Chem.*, 2001, **12**, 949; (*b*) N. V. Craynest, C. Santaella, O. Boussif and P. Vierling, *Bioconjugate Chem.*, 2002, **13**, 59.

